A&A 450, 1173–1179 (2006)
DOI: 10.1051/0004-6361:20053485

Astronomy & Astrophysics

Lithium abundances and rotational behavior for bright giant stars⋆,⋆⋆

A. Lèbre[1], P. de Laverny[2], J. D. do Nascimento Jr.[3], and J. R. De Medeiros[1,3]

[1] Groupe de Recherche en Astronomie et Astrophysique du Languedoc, UMR 5024/ISTEEM (CNRS), Université de Montpellier II, Place Bataillon, 34095 Montpellier, France
e-mail: lebre@graal.univ-montp2.fr
[2] Observatoire de la Côte d'Azur, Département Cassiopée, UMR 6202 (CNRS), BP 4229, 06304 Nice, France
[3] Departamento de Física, Universidade Federal do Rio Grande do Norte, 59072-970 Natal, RN, Brazil

Received 20 May 2005 / Accepted 16 November 2005

ABSTRACT

Aims. We study the links possibly existing between the lithium content of bright giant stars and their rotational velocity.
Methods. We performed a spectral analysis of 145 bright giant stars (luminosity class II) spanning the spectral range from F3 to K5. All these stars have homogeneous rotational velocity measurements available in the literature.
Results. For all the stars of the sample, we provide consistent lithium abundances ($A_{\rm Li}$), effective temperatures ($T_{\rm eff}$), projected rotational velocity ($v \sin i$), mean metallicity ([Fe/H]), stellar mass, and an indication of the stellar multiplicity. The gradual decrease in lithium abundance with $T_{\rm eff}$ is confirmed for bright giant stars, and it points to a dilution factor that is at least as significant as in giant stars. From the F to K spectral types, the $A_{\rm Li}$ spans at least three orders of magnitude, reflecting the effects of stellar mass and evolution on dilution.
Conclusions. We find that the behavior of $A_{\rm Li}$ as a function of $v \sin i$ in bright giant stars presents the same trend as is observed in giants and subgiants: stars with high $A_{\rm Li}$ are moderate or fast rotators, while stars with low $A_{\rm Li}$ show a wide range of $v \sin i$ values.

Key words. stars: abundances – stars: atmospheres – stars: evolution – stars: rotation

1. Introduction

Lithium is a key element in the study of the chemical evolution of the Galaxy, as well as in understanding the evolutionary history of stars, due particularly to its role as an important diagnostic of internal stellar mixing. In recent years, there has been a tremendous upsurge in the observational study of the stellar lithium line at 6707.81 Å in field stars at different regions in the Hertzsprung Russel diagram. The behavior of Li abundances as a function of effective temperature is now well-established for both subgiant stars (De Medeiros et al. 1997; Lèbre et al. 1999; Randich et al. 2000; Mallik et al. 2003) and giant stars (Brown et al. 1989; Wallerstein et al. 1994; De Medeiros et al. 2000; de Laverny et al. 2003).

These studies have shown, in the broadest sense, two clear distinct features in the distribution of Li abundances ($A_{\rm Li}$) along the spectral regions F, G, and K. Single subgiants and giants bluer than the ones of the spectral types F8 and G0, respectively, present a wide dispersion in $A_{\rm Li}$ from about null detection to the current interstellar medium and meteoritic observed value of about 3.2 dex. After a sudden decline around the referred spectral types, the abundances of lithium progressively decrease with effective temperatures once the stars evolve along the spectral types G to K. Qualitatively, such behavior reflects the dilution of surface lithium by convective mixing as a consequence of the development of the convective envelope toward the inner and hotter stellar regions, where Li is expected to be destroyed rapidly by (p, α) reactions at temperatures $>2.4 \times 10^6$ K. Thus, subgiant and giant stars evolving into the G and K spectral types are expected to have low lithium abundances. Moreover, theoretical models predict that surface lithium has to be diluted by a factor of 28 to 60 in stars of 1–9 $M_\odot$ at the bottom of the red giant branch (Iben 1965, 1966a,b, 1967).

After this stage, no additional convective dilution should occur. Nevertheless, the observational behavior of $A_{\rm Li}$ shows that the dilution factor is far more important than the standard theoretical predictions, with values as high as 1000 within the giant region (Brown et al. 1989; De Medeiros et al. 2000). This fact points to additional mixing mechanisms operating in evolved stars. From different studies (e.g.: Brown et al. 1989; Fekel & Balachandran 1993; Drake et al. 2002) there is now a growing list in the literature of single G- and K-type giant stars

⋆ Based on observations collected at ESO, La Silla, Chile, and at the Observatoire de Haute Provence, France, operated by the Centre National de la Recherche Scientifique (CNRS).
⋆⋆ Table 1 is only available in electronic form at http://www.edpsciences.org

that violate this general rule, exhibiting $A_{\rm Li}$ far in excess of the predicted values. The root-cause for such unexpected behavior is not understood clearly.

In addition to the behavior of lithium versus effective temperature, the relationship between $A_{\rm Li}$ and the rotational velocity in subgiant and giant stars has been studied by different authors (Wallerstein et al. 1994; De Medeiros et al. 1997, 2000; do Nascimento et al. 2000, 2003; de Laverny et al. 2003; Mallik et al. 2003). In spite of the fact that fast rotators present enhanced lithium content, the connection rotation-lithium seems to be more complex and to depend on different stellar parameters. Slow rotators, e.g. typically giants and subgiants with $v \sin i$ lower than about $10.0\,{\rm km\,s^{-1}}$, show a wide range of $A_{\rm Li}$ values with at least 3 mag of dispersion (De Medeiros et al. 2000; do Nascimento et al. 2003; de Laverny et al. 2003). Such dispersion apparently depends on stellar mass (De Medeiros et al. 2000).

For stars of higher luminosity classes, namely for bright giants and supergiants, previous investigations of the behavior of lithium and its connection to rotation have been hampered by the paucity of data. Luck & Wepfer (1995) have analyzed the behavior of $A_{\rm Li}$ for a sample of 38 field bright giants of spectral types F, G and K. In spite of the limitation of their sample composed of 13 F-type, 22 G-type, and 3 K0 bright giants, these authors have observed, for this luminosity class, the well-known gradual decrease in $A_{\rm Li}$ with effective temperature established for other luminosity classes. Luck & Wepfer (1995) have also found that Li depletions for bright giants are more severe than theoretical predictions with a dilution factor between 100 and 1000.

With the main goal of settling the question of the behavior of lithium and its connection to rotation in evolved intermediary-mass stars, we here present a spectroscopic study of the lithium line at 6707.81 Å for a large sample of bright giants with spectral types from middle F to middle K. For all these stars, precise radial and rotational velocity measurements ($v_{\rm rad}$ and $v \sin i$) are available from De Medeiros & Mayor (1999). The combination of our spectroscopic data with these $v \sin i$ measurements allows an unprecedented analysis of the connection rotation-lithium for intermediate-mass bright giant stars. Furthermore, this set of data ($A_{\rm Li}$ and $v \sin i$ measurements) is used for the study of possible links to the other properties of bright giant stars, such as metallicity, stellar mass, and binarity. In the next section (Sect. 2) we present our program sample and the spectroscopic observations we have collected. Section 3 describes the chemical analysis performed on our 145 bright giants in order to derive their stellar parameters and Li abundances. The main conclusions on the Li behavior along rotational velocity, effective temperature, indication of binarity, and stellar evolution are finally drawn in the last section (Sect. 4).

2. Data description

2.1. The working sample

For the present study, we composed our observational sample from a selection of 145 F, G and K bright giants in the catalog of rotational and radial velocities by De Medeiros & Mayor (1999). Let us recall that this work compiles precise rotational velocity $v \sin i$ and signatures of either single or binary behavior for a large and homogeneous sample of about 430 bright giants. The rotational velocities measured by these authors have an uncertainty of about $2.0\,{\rm km\,s^{-1}}$ for stars with a $v \sin i$ lower than about $30.0\,{\rm km\,s^{-1}}$. For faster rotators, the estimations indicate an uncertainty of about 10% on the measurements of $v \sin i$.

Stars in our observational sample were selected to cover the spectral range from F3 to K5 in the luminosity class II. Such a selection ensures that we can focus on 3 regions: (i) the region where bright giants present a broad range in values of rotational velocity (the F-type stars), (ii) the region of the discontinuity in rotation (the late F-type/early G-type stars), and (iii) the region of the slow rotators (the G- and K-type stars). Table 1 lists the 145 program stars in order of increasing HD number, with the respective projected rotational velocity $v \sin i$ from De Medeiros & Mayor (1999) and the stellar parameters derived from the spectroscopic study (see next section).

2.2. Spectroscopic observations

The data were acquired during three observational runs in August 1997, February 1998, and July 2003 for northern stars, and in November 1997 for southern stars. We used three different telescopes and instrumentations to observe the spectral region around the lithium line at 6707.81 Å. For northern stars, high-resolution spectra of the lithium region were acquired with the AURELIE spectrograph (Gillet et al. 1994) mounted at the 1.52 m telescope of the Observatoire de Haute Provence (OHP, France). The spectrograph used a cooled 2048-photodiode detector forming a 13 μm pixel linear array. A grating with 1800 lines/mm was used, giving a mean dispersion of 4.7 Å/mm and a resolving power around 45 000 (at 6707 Å). For this instrument and the selected set-up, the spectral coverage was about 120 Å. The signal-to-noise ratio was always better than 50. In July 2003, complementary spectra (mainly of F type bright giant stars) were collected with the ELODIE spectrograph mounted at the 1.93 m telescope of the OHP (Baranne et al. 1996). Very similar instrumental conditions were used (resolving power of 42 000 and signal-to-noise ratio better that 50).

For southern stars, high-resolution spectra were acquired with the Coudé Echelle Spectrometer (CES) in the long camera mode (Kapper & Pasquini 1996), mounted at the 1.44 m CAT telescope, at La Silla, ESO. An RCA high resolution CCD with 640×1024 pixels was used as the detector with a pixel size of 15×15 μm. The dispersion was around 1.9 Å/mm and the resolving power was about 95 000 (at 6707 Å). The spectral coverage for this instrument was about 70 Å and the signal-to-noise ratio was always better than 80.

For all the observational runs, thorium lamps were observed before and after each stellar observation for wavelength calibration, whereas 3 series of flat-field using an internal lamp of tungsten were obtained during each night of observation.

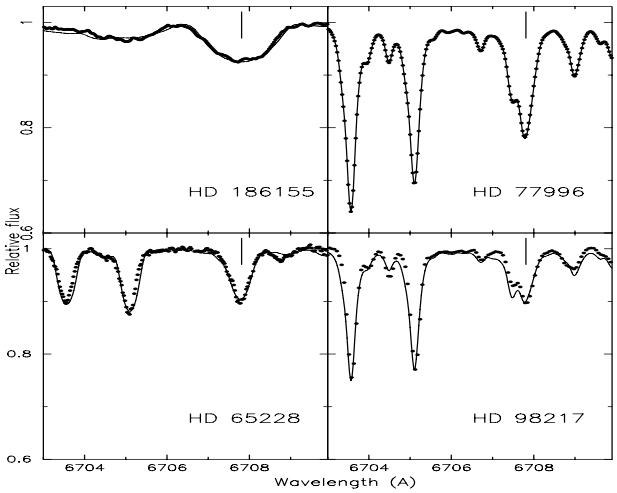

Fig. 1. Lithium spectral region for four program stars that present moderate to high Li abundances. In each panel, the observed spectrum is the dotted line, while the thin line indicates the synthetic spectrum computed with the stellar parameters mentioned in Table 1 for the relevant star. The Li I 6707.81 Å line is indicated with a short vertical line.

Flat-field corrections and wavelength calibrations were performed using the MIDAS package.

3. Stellar parameters and lithium abundances

3.1. Adopted methodology

For our present spectroscopic analysis and in order to stay consistent with our previous works, we derived LTE lithium abundances ($A_{\rm Li}$) from the resonance line at 6707 Å using the spectrum synthesis method (see Lèbre et al. 1999; and Jasniewicz et al. 1999, for more details). To compute the most appropriate synthetic spectra to fit the observations, a first guess for the stellar parameters of our list of bright giants was estimated. We thus looked into the literature to find effective temperatures ($T_{\rm eff}$), gravities ($\log g$), and often metallicities ([Fe/H]), mainly in Cayrel de Strobel et al. (2001), in Allende Prieto & Lambert (1999), and in Alonso et al. (1999). For sample stars without any published stellar parameters, we first estimated $T_{\rm eff}$ from $(B-V)$ color index (Flower 1996) and set $\log g = 2.0$, a microtuburlence velocity of 2 km s^{-1} and [Fe/H] = 0.0, those values being commonly adopted for Pop. I giant stars.

Synthetic spectra were then computed from these stellar parameters and with $v \sin i$ from De Medeiros & Mayor (1999). We used the same line list and model atmospheres as described in Lèbre et al. (1999) and in Jasniewicz et al. (1999). The stellar parameters of all the bright giants (mainly $T_{\rm eff}$, [Fe/H], and $\log g$) were then corrected, when necessary, in order to improve the fit quality of the several Fe I and other metallic lines found in the observed spectral range (~120 Å) centered on the Li line feature. The final adopted stellar parameters and the derived Li abundances are presented in Table 1 (online material) for all the stars of our sample. For four selected stars, in Fig. 1, we present their spectra in the Li region (observation and the best fit as synthetic spectrum).

Table 2. Comparison of measured $A_{\rm Li}$ and fundamental parameters for 18 program stars in common with Luck & Wepfer (1995). While for these stars our measured values are listed in Table 1, the present table displays the atmospheric parameters and Li abundances ($A_{\rm Li}$) spectroscopically derived by Luck & Wepfer (1995). The differences in $T_{\rm eff}$ ($\Delta T_{\rm eff}$) and in $A_{\rm Li}$ ($\Delta A_{\rm Li}$) present rms of 100 K and 0.35 dex, respectively. No value (–) in the column $\Delta A_{\rm Li}$ means that we derived upper limit in $A_{\rm Li}$ in agreement with the value reported in Luck & Wepfer (1995).

HD	$T_{\rm eff}$	$\log g$	[Fe/H]	$A_{\rm Li}$	$\Delta A_{\rm Li}$	$\Delta T_{\rm eff}$
1227	5075	2.7	0.05	0.76	>0.36	–25
27022	5275	2.6	0.05	1.25	0.35	5
65228	5900	1.7	0.16	2.52	0.4	–300
67447	4825	1.5	–0.08	1.15	0.05	–175
68752	4725	0.8	–0.14	<–0.23	–	25
71115	5050	2.2	–0.03	0.80	>0.4	–100
76219	4875	1.9	0.00	0.31	–	–125
76494	4900	2.0	0.01	1.00	0.60	–50
109379	5125	2.2	0.02	1.03	0.13	–25
129989	4800	2.2	0.16	–0.03	–	0
150030	4775	1.9	0.03	0.26	–	–125
161149	6650	3.0	0.42	2.27	>0.27	30
173009	4500	1.0	–0.30	–0.09	–	0
180809	4500	1.6	0.09	0.07	–	0
195295	6525	1.9	0.05	1.84	>0.34	–75
197177	5150	2.3	0.47	1.37	0.47	0
214567	5050	2.5	–0.11	<–0.26	–	–50
216756	6725	3.9	–0.09	3.05	–0.05	75

As already discussed by Lèbre et al. (1999), the major source of uncertainty for this abundance analysis comes from errors in the determination of the $T_{\rm eff}$. We estimated that effective temperatures, issued from synthetic spectra, were derived with a smaller uncertainty than ±200 K. This leads to an error of less than 0.2 dex on the derived metallicities and lithium abundances.

3.2. Comparison of our measured $A_{\rm Li}$ to previous studies

There is up to now only one study in the literature that is fully devoted to lithium abundances in intermediate-mass, evolved stars including bright giants (Luck & Wepfer 1995). Nevertheless, this study is based on a limited sample of 38 bright giant stars. Fundamental parameters and $A_{\rm Li}$ values were derived by these authors following a synthesis procedure based on MARCS models, then comparable to the procedure we have adopted here. Hence we present a comparison of the derived parameters for 18 stars common to both programs. As shown in Table 2 our data agree rather well with those from Luck & Wepfer (1995), considering the error bars in both works. In this context, both data sets ideally complement each other from the blue to the red spectral regions. The difference in $T_{\rm eff}$ computed for the 18 stars presents a rms of 100 K. The difference in $A_{\rm Li}$ has been computed only for Li detection in both works (11 stars among 18), thereby excluding upper limits on $A_{\rm Li}$. It presents an rms of 0.35 dex. For individual cases, however there are some

puzzling differences in $T_{\rm eff}$ (HD 65228, explaining entirely its disagreement on $A_{\rm Li}$), in [Fe/H] (HD 27022, HD 197177), or in $A_{\rm Li}$ (HD 76494, HD 161149). For those last two stars, the difference in $A_{\rm Li}$ clearly comes from the adopted $v \sin i$ values in both works. Indeed, Luck & Wepfer (1995) used fairly inaccurate and non-homogeneous $v \sin i$ values (coming from the Bright Stars Catalogue, or not even determined for a few stars), while our synthetic spectra are computed with highly accurate $v \sin i$ values obtained from CORAVEL measurements (De Medeiros & Mayor 1999). For the 18 common stars, we then computed synthetic spectra with atmospheric parameters, Li content, and $v \sin i$ values as presented in Luck & Wepfer (1995). They clearly failed to match our own observations and their Li feature, mainly due to a deficiency of the line broadening in the synthetic spectra. Thus we feel more confident of our own determination of atmospheric parameters and $A_{\rm Li}$ (as presented in Table 1).

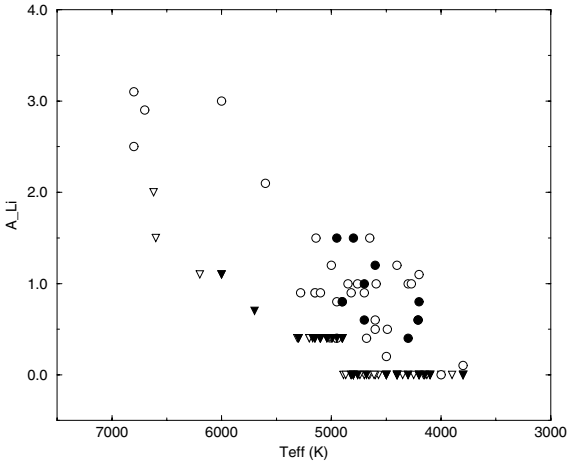

Fig. 2. Lithium abundances versus effective temperature. Single and binary stars are indicated with open and filled symbols, respectively. Triangles and circles refer to our present Li analysis, triangles being for Li upper limits, while circles are for Li abundance determinations. Effective temperatures were derived with a smaller uncertainty than 200 K, leading to an error of less than 0.2 dex on lithium abundances.

4. Results and discussion

In addition to the unprecedented list of precise lithium abundances for 145 bright giant stars along the spectral range F, G, and K, the present work offers a unique possibility to study the lithium content in intermediate-mass, evolved stars of population I and its link with relevant stellar parameters.

4.1. Lithium abundance versus effective temperature

For the analysis of $A_{\rm Li}$ as a function of effective temperature, we followed two different approaches: the standard one on the basis of the $A_{\rm Li}$ versus $T_{\rm eff}$ plan, and a second one based on the position of stars in the HR diagram. The latter is clearly more solid, giving the behavior of $A_{\rm Li}$ versus $T_{\rm eff}$ as a function of mass.

Figure 2 shows lithium abundances as a function of effective temperature for the bright giant stars of our sample (represented by circles and by triangles for upper limit measurements). In this figure (and also in subsequent ones) open symbols stand for single stars, whereas filled symbols indicate binaries (or stars with variability in radial velocity). The gradual decrease in lithium abundance with effective temperature for bright giant stars is solidly defined in Fig. 2, perhaps pointing to a dilution factor at least as important as in giants. Following the same trend observed in giant stars (De Medeiros et al. 2000; De Laverny et al. 2003), Fig. 2 shows that at a given effective temperature, all along the F to K spectral types, the $A_{\rm Li}$ spans about three orders of magnitude or more, reflecting the effects of the evolutionary stage and stellar mass on dilution (e.g.: Lambert et al. 1980; Brown et al. 1989). These features are clearly observed in Fig. 3, where mass and evolutionary effects are taken into consideration (see next section). The absence of stars in the $T_{\rm eff}$ interval from 5500 K to 6500 K corresponds to the Hertzsprung gap.

4.2. Lithium abundance in the $T_{\rm eff}$– luminosity diagram

We turn now to the analysis of the $A_{\rm Li}$ behavior in the $T_{\rm eff}$ versus luminosity diagram. To infer the evolutionary status of our sample stars, their absolute magnitudes were first calculated from V magnitudes and parallaxes given in the Hipparcos catalog (Perryman et al. 1997) available at SIMBAD/CDS. Then the stellar luminosities were derived from these absolute magnitudes using a bolometric correction (BC) interpolated between giants and supergiants as described in Flower (1996). We used evolutionary tracks at solar metallicity and mass range between 1.5 to 9 $M_{\odot}$, taken from grids of stellar models provided by Schaller et al. (1992). Hence the mass of each bright giant can be estimated with respect to these theoretical evolutionary tracks. Note that 6 stars listed in Table 1, but without available HIPPARCOS parallaxes, have been excluded from these diagrams in order to ensure consistency in the estimation of the evolutionary status of the largest part of our sample.

Figures 3 and 4 display such HR diagrams, indicating the lithium abundances and rotational velocity, respectively, where the effects of mass and evolution can be outlined. In these figures the symbol sizes are proportional to the values of relevant parameters, respectively $A_{\rm Li}$ and $v \sin i$. The location of the turn-off is indicated with a dotted line, while the location of the bottom of the red giant branch is indicated with a dashed line. From these figures a first important feature of the evolutionary status of the present sample should be underlined: the large majority of our sample stars is located in the mass range expected for bright giants, which have masses from about 2.5 $M_{\odot}$ to 9 $M_{\odot}$, although a few stars are found with smaller masses than about 2 $M_{\odot}$. Although these objects are classified in the literature as bright giants, they are clearly rather evolving around the turn-off or at the main sequence. Another important point concerns the evolutionary status of the bright giants, namely those stars with masses larger than about 2.5 $M_{\odot}$: stars with effective temperature smaller than about 5000 K (or $\log(T_{\rm eff}) < 3.7$) may be found on different evolutionary stages, evolving either in the first crossing on the giant branch or evolving along blue–loops.

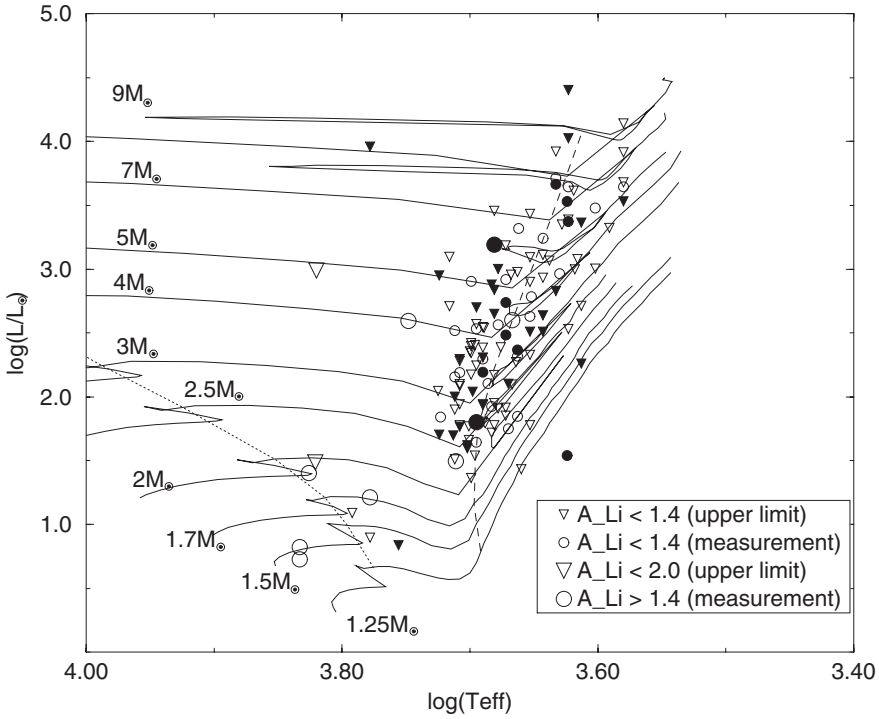

Fig. 3. Hertzsprung-Russell diagram of our program stars with evolutionary tracks from Schaller et al. (1992). The location of the turn-off is indicated with a dotted line, while the location of the bottom of the red giant branch is indicated with a dashed line. Single stars and binaries are represented by open and filled symbols, respectively. Indication of the lithium abundances ($A_{\rm Li}$) is given through two different symbol sizes ($A_{\rm Li}$ inf./sup. to 1.4 dex). Upper limits on $A_{\rm Li}$ are also indicated with open/filled triangles. See text (Sect. 4.2) for more details.

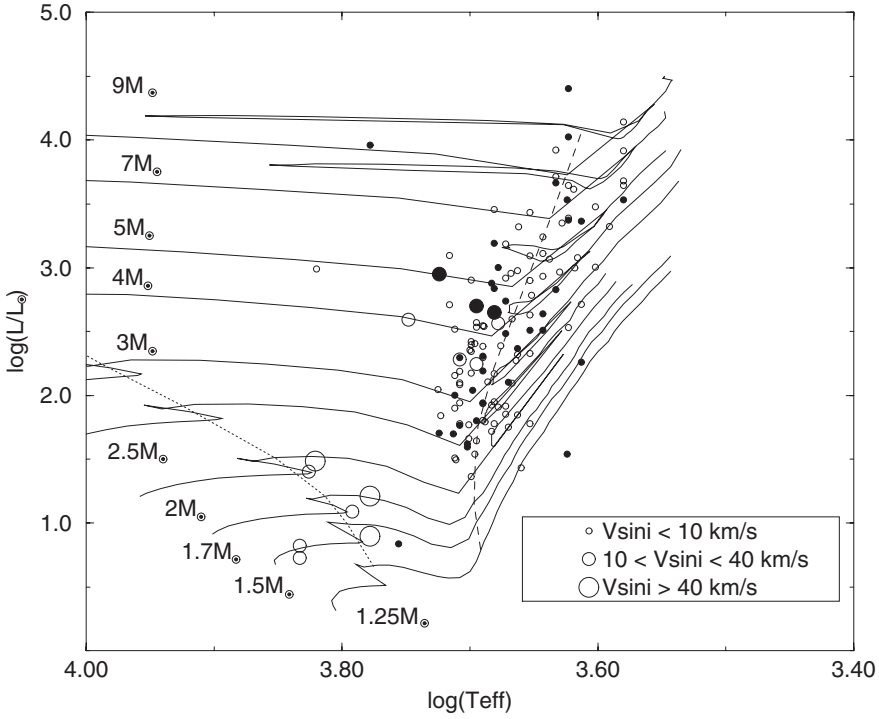

Fig. 4. Same as Fig. 3, but the symbol sizes refer to rotational velocity (as indicated in the legend frame). Again, binaries are represented by filled symbols.

From Fig. 3, we notice that the low mass stars (namely stars with $M < 2\ M_{\odot}$), present the expected behavior for their $A_{\rm li}$: stars located in the F spectral region (those around the turn-off) show a wide range in $A_{\rm li}$, from about the cosmic value $A_{\rm Li} \sim 3.2$, to abundances lower than 0.0., whereas stars along the G to K spectral range, except for a very few

$A_{\rm Li}$ moderate values, present essentially low lithium content. For typical bright giants (i.e., stars in the mass range 2.5 $M_{\odot}$ to 9 $M_{\odot}$), the $A_{\rm Li}$ behavior follows – at least qualitatively – the same feature as has already been observed for giant and subgiant stars (De Medeiros et al. 2000; De Laverny et al. 2003; do Nascimento et al. 2000). There is indeed a trend to a large range of $A_{\rm Li}$ values among stars located on the blue side of the Hertzsprung gap, while the large majority of stars on the red side (namely in the G to K spectral regions) presents essentially low Li abundances. Moreover, in this latter spectral region, single and binary stars seem to follow the same behavior. Brown et al. (1989) have shown that giant stars with average masses around 1.2 $M_{\odot}$ have average $A_{\rm Li} < 0.0$, corresponding to 1.5 dex less than abundances predicted by standard theory. The present work shows the same striking feature among giant stars with larger masses than about 2 $M_{\odot}$. Indeed ~70% of our sample stars show $A_{\rm Li} < 0.4$, and ~40% even show $A_{\rm Li} < 0.0$. Following the similar analysis undertaken by Brown et al. (1989), we found that Li abundance correlates poorly with the mass of bright giant stars.

Despite these clear results, determination of the Li dilution factor for the bright giant stars is not an evident task. As we have underlined, stars with effective temperature that is smaller than about 5000 K are in different evolutionary stages, even if they have well-developed convective envelopes. As shown by different authors (e.g.: do Nascimento et al. 2003) after the F-late type spectral region, corresponding to effective temperatures that are smaller than about 5000 K, the development in mass of the convective envelope arises very rapidly. For the stars evolving on the first crossing, convective dilution associated with some extra-mixing process is expected to represent the main root-cause to explain the observed low $A_{\rm Li}$ abundances. Nevertheless, for stars evolving on the blue-loops one may expect a more complex status. Certainly, these stars have experienced mixing, even quite deeply, and their primordial surface Li content should be as diluted so as in stars on the first crossing or more. In addition, mass-loss in stars evolving along the loops is expected to be more severe than in giants on the first crossing. This process should also play a role in the increase of Li content at the stellar surface. In this context, the Li dilution factor strongly depends on the evolutionary status of the stars.

However an additional interesting point in the present survey is the apparent lack of lithium-rich bright giant stars, typically single late G- and K-type stars with $A_{\rm Li}$ as large as the cosmic lithium abundance value. In spite of this fact, few bright giants present a moderate content of lithium. Two binaries, HD 34579 and HD 77996, and two single stars, HD 41927 and HD 98217, are all low rotators and, in the spectral type range G8II to K2II, show slightly enhanced Li content, with $A_{\rm Li} \sim 1.5$ dex.

4.3. Lithium abundance versus rotational velocity

For bright giants, the distribution of their $v \sin i$ values as a function of effective temperature presents a sudden discontinuity around $T_{\rm eff} \sim 5200$ K, corresponding to the spectral type around F9II (De Medeiros 1989). In Fig. 4, this feature is again clearly observed for our sample of stars. Indeed, binary and single stars that are hotter than ~5200 K show a wide range of rotational velocity, with $v \sin i$ ranging from low to moderate and to high rotators, while on the cooler side of the discontinuity, except for a few moderate rotators with $v \sin i$ between 10 and 20 km s^{-1}, single and binary stars present essentially low $v \sin i$ ($v \sin i < 10$ km s^{-1}).

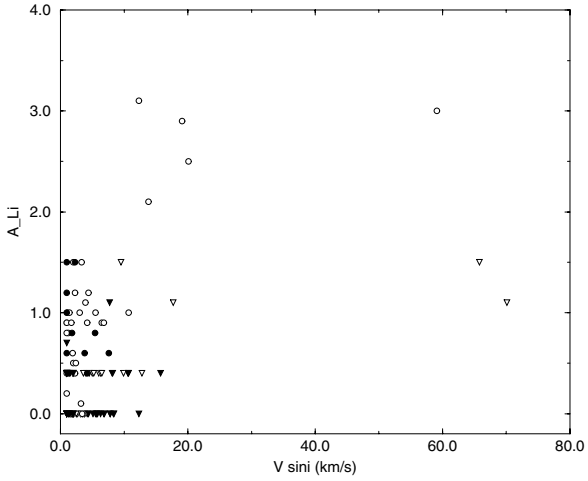

Fig. 5. Lithium abundances versus rotational velocity. Single and binary stars are indicated with open and filled symbols, respectively. Triangles and circles refer to our Li abundance determinations, triangles being for $A_{\rm Li}$ upper limits. We estimated the error on lithium abundances of less than 0.2 dex. The rotational velocities have an uncertainty of about 2.0 km s^{-1} for low and moderate rotators ($v \sin i$ lower than about 30.0 km s^{-1}) while for fast rotators, the estimations indicate an uncertainty of about 10% on the measurements of $v \sin i$.

Finally, Fig. 5 shows the behavior of $A_{\rm Li}$ as a function of $v \sin i$. For the first time, it is then possible to establish this behavior on a large sample of bright giants with homogeneous and high precision $v \sin i$ measurements. Indeed, we have strictly limited the representation of Fig. 5 to our program stars in order to ensure the homogeneity of the displayed data: $v \sin i$ values from CORAVEL measurements and $A_{\rm Li}$ determinations from our present spectroscopic study. The same trend already observed for giant and subgiant stars (De Medeiros et al. 2000; De Laverny et al. 2003; do Nascimento et al. 2000) is present here: stars with high $A_{\rm Li}$ ($A_{\rm Li} > 2.0$ dex) are moderate or fast rotators ($v \sin i > 10$ km s^{-1}), whereas for low $A_{\rm Li}$ there is a large spread in the values of $v \sin i$. Nevertheless, two fast rotators, HD 161149 and HD 168393 seem to stand out of such a trend, presenting rather low Li content. These stars appear to have no particularity, except the fact that, in the context of the present sample, they are rather low mass stars evolving near the turn-off.

5. Conclusions

In this work, we present an unprecedented list of precise stellar parameters and lithium abundances for 145 bright stars ranging along the spectral types F, G, and K, the large majority of them genuine bright giants, inferred from spectroscopic

analysis based on MARCS models. This study of lithium content in intermediate-mass, evolved stars of Population I (i.e., with stellar mass ranging from 2.5 $M_{\odot}$ to 9 $M_{\odot}$) complements the only work ever produced on bright giants (Luck & Wepfer 1995) and also similar studies devoted to lower luminosity class stars: subgiants (Lèbre et al. 1999; do Nascimento et al. 2000) and giants (De medeiros et al. 2000; De Laverny et al. 2003).

Considering the behavior of $A_{\rm Li}$ as a function of effective temperature, the gradual decrease in lithium abundance with effective temperature is again well-established for bright giant stars, pointing to a dilution factor that is at least as important as in giants. This behavior follows the same trend already observed in giant and subgiant stars: at a given effective temperature, all along the F to K spectral types, the $A_{\rm Li}$ spans at least three orders of magnitude, reflecting the effects of evolutionary status and stellar mass on dilution.

For single stars, as well as for binaries, there is also a large dispersion on $A_{\rm Li}$ values for stars located on the blue side of the Hertzsprung gap, while almost all the stars located on the red side (G to K spectral type range) present low Li abundances. This behavior follows the one found in previous works for giants of smaller stellar masses. We show here that bright giant stars with larger masses than about 2.0 $M_{\odot}$ have $A_{\rm Li} < 0.0$, corresponding to at least 1.5 dex less than abundances predicted by standard theory. We also found that Li abundance correlates poorly with the mass of bright giant stars. While our survey points to an apparent lack of lithium-rich stars (typically single late G- and K-type stars, with $A_{\rm Li}$ as large as the cosmic value), we detected, however, four genuine bright giants (low rotators and in the spectral type range G8II to K2II), showing enhanced Li content (with $A_{\rm Li} \sim 1.5$ dex).

Considering the behavior of $A_{\rm Li}$ as a function of rotational velocity, we find the same trend for our sample of bright giants that has already been observed for giant and subgiant stars: stars with high $A_{\rm Li}$ are moderate or fast rotators, while stars with low $A_{\rm Li}$ present a large spread in the values of $v \sin i$.

Finally, the present work indicates that some related observational programs should be undertaken in order to have a more solid understanding of the Li behavior in evolved stars from low to intermediate masses. First, the determination of Li abundances for a large sample of stars evolving at and immediately after the turn-off – in particular for intermediate mass stars – will help us quantify the level of Li content in stars leaving the main sequence. Secondly, the determination of Li content in G and K supergiants is also welcome, because it will be possible to enlarge the present available sample of evolved stars. Thirdly, the determination of carbon isotope ratios in G and K giant and bright giant stars is an additional required step, since this ratio is a very sensitive diagnostic of stellar evolution. All these data are of fundamental importance for further understanding the Li dilution once stars of low to intermediate masses leave the main sequence and begin the ascent to the red giant branch.

Acknowledgements. This work was supported by continuous grants from CNPq Brazilian Agency, by a PRONEX grant of the FAPERN Rio Grande do Norte Agency, and by financial resources from the French CNRS/INSU Programme National de Physique Stellaire (PNPS). J.D.N.Jr acknowledges the CNPq Brazilian support CNPq/PROFIX 540461/01-6. The authors warmly thank Dr. G. Wallerstein for his fruitful comments on the paper. This research has made use of the SIMBAD database, operated at the CDS (Strasbourg, France), and of NASA's Astrophysics Data System.

References

Allende Prieto, C., & Lambert, D. L. 1999, A&A, 352, 555
Alonso, O., Arribas, S., & Martìnez-Roger, C. 1999, A&AS, 139, 335
Baranne, A., Queloz, D., Mayor, M., et al. 1996, A&AS, 119, 373
Brown, J. A., Sneden, C., Lambert, D. L., & Dutchover, E. 1989, ApJ, 71, 293
Cayrel, G., Soubiran, C., & Ralite, N. 2001, A&A, 373, 159
De Laverny, P., do Nascimento, J. D. Jr., Lèbre A., & De Medeiros, J. R. 2003, A&A, 410, 937
De Medeiros, J. R. 1989, Ph.D. Geneva Observatory
De Medeiros, J. R., do Nascimento, J. D. Jr., & Mayor, M. 1997, A&A, 317, 701
De Medeiros, J. R., & Mayor, M. 1999, A&AS, 139, 443
De Medeiros, J. R., do Nascimento, J. D. Jr., Sankarankutty, S., Costa, J. M., & Maia, M. R. G. 2000, A&A, 363, 239
do Nascimento, J. D. Jr., Charbonnel, C., Lèbre, A., De Laverny, P., & De Medeiros, J. R. 2000, A&A, 357, 931
do Nascimento, J. D. Jr., Cantos Martins, B. L., Melo, C. H. F., Porto de Mello, G., & De Medeiros, J. R. 2003, A&A, 405, 723
Drake, N. A., de La Reza, R., da Silva, L., & Lambert, D. L. 2002, AJ, 123, 2703
Fekel, F. C., & Balachandran, S. 1993, ApJ, 403, 708
Flower, P. J. 1996, ApJ, 469, 355
Gillet, D., Burnage, R., Kolher, D., et al. 1994, A&AS, 108, 181
Iben, I. J. 1965, ApJ, 142, 1447
Iben, I. J. 1966a, ApJ, 143, 483
Iben, I. J. 1966b, ApJ, 143, 505
Iben, I. J. 1967, ApJ, 147, 624
Jasniewicz, G., Parthasarathy, M., de Laverny, P., & Thèvenin, F. 1999, A&A, 342, 831
Kapper, L., & Pasquini, L. 1996, CAT+CES Operating Manual, ESO report, 3P6CAT-MAN-0633-0001
Lambert, D. L., Dominy, J. F., & Sivertsen, S. 1980, ApJ, 235, 114
Lèbre, A., De Laverny, P., De Medeiros, J. R., Charbonnel, C., & Da Silva, L. 1999, A&A, 345, 936
Luck, R. E., & Wepfer, G. G. 1995, AJ, 110, 2425
Mallik, S. V., Parthasarathy, M., & Pati, A. K. 2003, A&A, 409, 251
Perryman, M. A. C., Lindegren, L., Kovalesky, J., et al. 1997, A&AS, 323, 49
Randich, S., Pasquini, L., & Pallavicini, R. 2000, A&A, 356, L25
Schaller, G., Schaerer, D., Meynet, G., & Maeder, A. 1992, A&AS, 96, 269
Wallerstein, G., Bohm-Vitense, E., Vanture, A. D., & Gonzalez, G. 1994, AJ, 107, 2211

Online Material

Table 1. List of our 145 program stars with their main parameters. The $(B-V)$, $v_{\rm rad}$, $v \sin i$, and binarity index are from De Medeiros & Mayor (1999), and $T_{\rm eff}$, $\log g$, [Fe/H], and $A_{\rm Li}$ are from our chemical analysis based on synthetic spectra (see Sect. 3.1). Stars indicated with an asterisk (*) have also been observed by Luck & Wepfer (1995) and comparisons on atmospheric parameters and $A_{\rm Li}$ are discussed in Sect. 3.2. Stars indicated with such a symbol (⁻) are not included in Figs. 3 and 4 (HR diagrams) as there is no HIPPARCOS parallax available for these six objects (see Sect. 4.2).

Star	Sp. Type	$B-V$	$v_{\rm rad}$ km s^{-1}	$v \sin i$ km s^{-1}	Binarity	$T_{\rm eff}$ K	$\log g$	[Fe/H]	$A_{\rm Li}$
HD 936	G7.5II	1.12	0.14	8.1	sb	4900	2.0	–0.3	<0.4
HD 1227*	G8II-III	0.92	0.30	1.0	–	5100	2.6	0.0	<0.4
HD 1367	K0II	0.94	–9.95	1.0	–	5150	2.0	0.0	<0.4
HD 1375	G8II	0.97	–0.45	1.0	–	5020	2.0	–0.2	<0.4
HD 4482	G8II	0.99	–5.11	1.0	sb	5040	2.0	–0.1	<0.4
HD 5418	G8II	0.96	5.03	1.0	–	5020	2.0	0.0	<0.4
HD 5848	K2II-III	1.21	7.89	1.0	–	4500	2.4	0.0	<0.0
HD 8681	K1II	1.12	–9.5	2.0	sb	4680	2.0	–0.4	<0.0
HD 11668	K0II	1.03	17.4	1.8	–	4800	2.0	–0.4	<0.0
HD 12409	G6II	0.91		6.0	–	5200	2.0	0.0	<0.4
HD 13280⁻	K1/K2II	1.20		3.0	–	4570	2.0	–0.4	<0.0
HD 13611	G6II-III	0.88	–4.36	1.5	sb	5100	2.0	0.0	<0.4
HD 13640⁻	K1/K2II	1.20		2.0	–	4570	2.0	–0.4	<0.0
HD 16735	K0II-III	1.12	–14.37	1.0	–	4820	2.0	–0.1	0.9
HD 16899	K0II	1.08	19.1	2.0	sb	4900	2.0	–0.5	<0.4
HD 17346	G9II	1.23	–7.00	2.7	–	4800	2.0	–0.3	<0.0
HD 18175	K0II	1.14	–34.67	<1.0	–	4680	3.0	–0.2	0.4
HD 20644	K2II-III	1.55	–3.92	1.4	sb	4150	2.0	0.0	<0.0
HD 21754	K0II-IIIFe	1.11	16.79	<1.0	sb	4700	2.6	–0.2	1.0
HD 21901	K1II	1.18		2.0	–	4570	2.0	–0.4	<0.0
HD 22287	G8II	0.97	33.0	2.0	–	4970	2.0	–0.4	<0.4
HD 24107	K1II	1.11	39.23	<1.0	–	4700	2.0	–0.4	<0.0
HD 25189	K2II-III	1.20	10.2	2.0	–	4600	2.0	–0.2	0.5
HD 25877	G8II	1.11	–13.03	4.5	–	4950	2.0	–0.1	<0.4
HD 26004	K0II-III	1.20	–12.1	2.0	–	4700	2.0	0.5	<0.0
HD 26045	K1II	1.14		2.0	–	4650	2.0	–0.2	<0.0
HD 26311	K1II-III	1.41	18.73	1.0	sb	4600	2.0	–0.2	1.2
HD 26673	G5II	1.01	–17.58	10.6	sb	4950	2.0	–0.1	<0.4
HD 27022*	G5II	0.82	–19.75	1.0	–	5280	2.5	–0.2	0.9
HD 30031	K2/K3II	1.35	–15.9	1.9	–	4600	2.0	–0.3	0.6
HD 30504	K4II	1.45	–25.24	1.6	–	4100	2.0	–0.4	<0.0
HD 31398	K3II	1.49	17.38	3.8	–	4160	2.0	0.1	<0.0
HD 31767	K2II	1.37	14.85	1.1	–	4590	2.0	–0.3	1.0
HD 32068	K4II	1.15	–1.70	6.8	sb	4100	2.0	0.1	<0.0
HD 32356	K5II	1.38	–46.82	<1.0	sb	4100	2.0	–0.3	<0.0
HD 32406	K0II-III	1.21	15.07	3.0	–	4850	2.0	–0.3	1.0
HD 33239	G9II	1.09	–11.0	2.0	–	4760	2.0	0.5	<0.0
HD 34579	G8II-III	1.02	–52.05	<1.0	sb	4950	2.0	–0.2	1.5
HD 38871	K0.5II	1.04	11.7	1.8	sb	4900	2.0	–0.3	0.8
HD 39400	K2II	1.38	11.06	3.5	–	4250	1.5	–0.2	<0.0
HD 39632	G9II	1.40	12.17	7.8	–	4350	2.0	–0.1	<0.0
HD 40733	G8II	1.06	12.7	5.7	sb	4820	2.0	–0.4	<0.0
HD 40801	K0II	0.99	33.32	<1.0	–	5000	2.0	–0.3	<0.4
HD 41927	K2II-III	1.34	0.13	3.3	–	4650	2.0	0.0	1.5
HD 42351	K1II	1.35	–2.59	2.5	–	4500	2.0	–0.2	<0.0
HD 43335	K5II	1.56	42.95	2.1	–	4200	2.0	–0.2	<0.0
HD 45416	K1II	1.19	31.69	1.9	–	4500	2.0	–0.3	<0.0
HD 47475	K0II	1.15	14.3	5.5	–	4660	2.0	–0.3	<0.0
HD 49380	K3II	1.30	–16.91	<1.0	–	4500	2.0	–0.2	<0.0
HD 49778⁻	G8II	1.04	0.8	2.0	–	5000	2.0	–0.4	<0.4
HD 50337	G6II	0.90	22.1	12.3	sb	4800	2.0	–0.4	<0.0
HD 50716⁻	G6II	0.90	13.8	15.7	sb	5200	2.0	–0.2	<0.4
HD 51315⁻	K0II	1.15		2.0	–	5100	2.0	–0.2	<0.4
HD 52938	K3.5II	1.71	5.36	3.9	–	4200	2.0	–0.1	1.1

Table 1. continued.

Star	Sp. Type	$B-V$	$v_{\rm rad}$ km s^{-1}	$v \sin i$ km s^{-1}	Binarity	$T_{\rm eff}$ K	$\log g$	[Fe/H]	$A_{\rm Li}$
HD 54519	K5II	1.51	13.5	5.7	sb	4200	2.0	–0.1	<0.0
HD 54825	K0II	1.06	42.11	<1.9	–	4900	2.0	0.0	<0.4
HD 55751	K2II	1.19	36.35	<1.0	–	4500	2.0	–0.3	0.2
HD 57146	G0II	0.96	30.4	9.9	–	5200	2.0	0.0	<0.4
HD 59878	K0II	1.00	33.82	<1.0	sb	5300	2.0	0.1	<0.4
HD 61772	K3II	1.54	–0.08	2.0	–	4000	2.0	–0.1	<0.0
HD 63032	K5II	1.71	16.3	8.3	sb	4200	2.0	–0.2	<0.0
HD 63870	K1II	1.11	–0.3	2.0	–	4800	2.0	–0.2	<0.0
HD 64067	G5II	1.12	19.12	7.6	sb	4700	2.0	–0.2	0.6
HD 64320	K0II	1.24	22.6	2.4	–	4490	2.0	–0.5	0.5
HD 65228*	F7II	0.72	12.96	13.8	–	5600	3.0	0.0	2.1
HD 65662	K4II	1.55	23.8	2.3	–	4400	2.0	–0.4	1.2
HD 66812	G8II	1.01	13.9	10.6	–	4950	2.0	–0.4	<0.4
HD 67249	G5II	1.21	26.79	6.5	–	4700	2.0	–0.4	0.9
HD 67447*	G7II	1.04	–11.64	4.4	–	5000	2.0	0.0	1.2
HD 68752*	G5II	1.07	16.39	6.9	–	4700	2.0	–0.4	<0.0
HD 70555	K1II	1.42	31.8	3.8	–	4400	2.0	–0.3	<0.0
HD 71115*	G7II	0.93	15.26	<1.2	sb	5150	2.2	–0.1	<0.4
HD 73155	K1.5II	1.30	4.1	3.1	–	4600	2.0	–0.4	<0.0
HD 76219*	G8II-III	1.00	15.87	6.3	–	5000	2.0	–0.2	<0.4
HD 76494*	G8II-III	1.00	–11.48	4.6	–	4950	2.0	<–0.3	0.4
HD 77250	K1II-III	1.11	32.70	1.6	–	4740	2.0	–0.2	<0.0
HD 77996	K2II-III	1.19	23.36	2.3	sb	4800	2.0	0.0	1.5
HD 79698	G6II	0.85	5.3	8.2	–	5310	2.0	–0.1	<0.4
HD 80126	G8II	1.04	14.7	3.8	–	4890	2.0	–0.4	<0.0
HD 87238	K1II	1.11	6.9	1.2		4900	2.0	–0.4	0.8
HD 88009	G8II	1.07	–19.11	<2.5	–	4820	2.0	–0.4	<0.0
HD 89388	K3II	1.54	8.2	5.5	–	4300	2.0	0.0	1.0
HD 89682	K3II	1.60	12.9	2.0	–	4300	2.0	–0.4	<0.0
HD 91942	K3.5II	1.60	9.4	5.8	–	3800	2.0	0.0	<0.0
HD 95725	K1II	1.05	–11.79	<1.0	–	4870	2.0	–0.1	<0.0
HD 98217	G8II	0.93	–15.36	2.0	–	5140	2.0	–0.2	1.5
HD 98839	G8II	1.00	–2.36	4.0	–	5010	2.1	0.0	<0.4
HD 106057	K0II-III	0.96	–26.30	<1.0	–	5100	2.0	–0.2	<0.4
HD 109379*	G5II	0.89	–7.90	4.2	–	5150	2.0	–0.3	0.9
HD 119035	G5II	0.96	–19.43	<1.0	–	4900	2.0	–0.2	<0.4
HD 125728	G8II	0.92	29.48	<1.0	sb	5170	2.0	–0.3	<0.4
HD 129989*,–	K0II-III	0.97	–17.50	8.4	–	4800	2.2	0.0	<0.0
HD 130766	K3II	1.35	–13.81	1.0	sb	4400	2.0	–0.5	<0.0
HD 145931	K4II	1.46	–22.62	1.0	sb	4300	2.0	–0.3	<0.0
HD 148897	G8II	1.29	15.86	<1.9	sb	4400	1.5	–0.7	<0.0
HD 150030*	G8II	1.04	–16.89	3.6	–	4900	2.0	–0.2	<0.4
HD 156283	K3II	1.44	–26.17	1.3	–	4130	1.7	–0.2	<0.0
HD 156681	K4II-III	1.54	38.76	1.0	–	4150	2.0	–0.3	<0.0
HD 157999	K2II	1.48	–28.38	4.2	sb	4300	2.0	0.0	0.4
HD 159181	G2II	0.95	–21.56	10.7	sb	5300	1.4	0.3	<0.4
HD 161149*	F5II	0.43	–53.95	65.8	–	6620	2.0	?	<2.0
HD 168393	F5II	0.55	26.93	70.1	–	6000	2.0	?	<1.1
HD 171874	F6II	0.48	–48.93	17.7	–	6200	2.5	0.0	<1.1
HD 173009*	G8II	1.11	–9.12	5.1	sb	4500	1.0	0.0	<0.0
HD 173764	G5II	1.09	–15.27	7.8	sb	4760	2.0	–0.2	<0.0
HD 174980	K0II-III	0.95	0.44	1.0	–	5150	2.0	0.1	<0.4
HD 177249	G5II	0.86	7.30	5.0	–	5100	2.3	0.0	<0.4
HD 180262	G8II-III	1.07	–25.59	1.4	–	5000	2.0	–0.3	<0.4
HD 180656	K1II	1.05	–46.84	1.0	–	4800	2.0	–0.3	<0.0
HD 180809*	K0II	1.26	–28.02	3.5	–	4500	2.0	0.0	<0.0

Table 1. continued.

Star	Sp. Type	$B-V$	$v_{\rm rad}$ km s^{-1}	$v \sin i$ km s^{-1}	Binarity	$T_{\rm eff}$ K	$\log g$	[Fe/H]	$A_{\rm Li}$
HD 183912	K3II	1.09	–24.33	1.4	–	4270	2.0	–0.1	1.0
HD 184944	K0II-III	1.04	–45.31	1.0	sb	4210	2.0	0.0	0.6
HD 186155	F5II-III	0.43	–21.79	59.1	–	6000	3.0	0.0	3.0
HD 186791	K3II	1.51	–3.18	3.8	sb	4210	2.0	0.0	0.6
HD 186927	K0II-III	1.07	–21.79	1.0	–	4900	2.0	0.0	<0.4
HD 189276	K5II-III	1.58	3.79	1.7	–	3900	2.0	–0.1	<0.0
HD 190147	K1II-III	1.12	–1.06	1.0	–	4610	2.4	–0.2	<0.0
HD 192004	K3II-III	1.40	–19.99	3.4	–	4200	1.4	0.0	<0.0
HD 193092	K5II	1.65	–20.48	5.4	sb	4200	2.0	0.0	0.8
HD 193217	K4II	1.63	–19.02	3.4	–	4000	2.0	0.0	0.0
HD 195295*	F5II	0.40	–17.91	9.5	–	6600	3.0	0.0	<1.5
HD 195432	G0II	0.64	–24.85	12.8	–	5100	2.0	0.3	<0.4
HD 196321	K5II	1.61	–9.69	1.9	–	3800	2.0	–0.2	<0.0
HD 197177*	G8II	0.87	–26.21	1.7	–	5150	2.3	0.0	0.9
HD 199098	K0II	1.09	–29.49	10.7	–	4760	2.0	–0.4	1.0
HD 199612	G8II-III	1.05	–19.04	1.3	sb	4800	2.0	–0.3	<0.0
HD 201251	K4II	1.57	–26.83	6.3	sb	3800	2.0	0.0	<0.0
HD 202109	G8II-III	0.99	19.17	1.0	sb	4990	2.0	–0.1	<0.4
HD 204509	F4II	0.38	–22.66	19.1	–	6700	3.0	0.1	2.9
HD 205603	G8II	0.94	–6.49	1.0	–	4950	2.0	–0.3	0.8
HD 206731	G8II	1.00	1.45	5.2	–	4970	2.0	–0.3	<0.4
HD 210807	G7II-III	0.92	–16.66	6.5	–	5000	2.2	–0.1	<0.4
HD 211300	K0II-III	1.01	–3.27	1.0	–	5000	2.0	0.0	<0.4
HD 214567*	G8II	0.93	–18.80	1.0	sb	5100	2.5	–0.4	<0.4
HD 216219	G0II	0.65	–7.46	1.0	sb	5700	3.3	–0.4	<0.7
HD 216756*	F5II	0.40	–28.32	12.3	–	6800	3.7	0.0	3.1
HD 217673	K2II	1.50	–6.46	3.2	–	4400	2.0	0.0	<0.0
HD 218043	F4II	0.40	–10.46	20.1	–	6800	3.0	0.1	2.5
HD 218356	K0II	1.29	–27.71	4.4	sb	4400	1.8	–0.1	<0.0
HD 220102	F5II	0.60	–30.09	7.7	sb	6000	3.0	–0.5	<1.1
HD 220369	K3II	1.68	–10.77	3.2	–	3800	2.0	0.0	0.1
HD 221661	G8II	0.99	7.91	<1.0	–	5100	2.0	0.0	<0.4
HD 223173	K3II	1.63	–5.40	4.2	–	3800	2.0	0.0	<0.0
HD 224870	G7II-III	0.97	–20.31	6.8	–	5100	2.0	-0.1	0.9
HD 225292	G8II	0.95	13.00	<1.0	sb	5040	2.0	–0.4	<0.4